Fracture behaviour testing of cementitious interfaces in mode I, II, III

C.H.Surberg
Corporate Research, Materials & Mechanics Department, Hilti Co., Principality of Liechtenstein

E.K.Tschegg
Institute of Applied and Technical Physics, Vienna University of Technology, Austria

ABSTRACT: The analysis of the fracture behaviour of homogenous and heterogenous materials under static load in modes II and III is a still unsolved problem in the field of material science. From literature reviews it can be seen that generally scientifically sound experimental determinations of the fracture behaviour in mode II and mode III, respectively, are still lacking. This is true for simple and complex sample geometries as well as loading devices. This paper presents testing methods which are based on simple sample geometries and loading devices. Furthermore, these testing methods were used to determine experimentally the interface bond characteristics between different types of aggregates and mortars in various fracture modes I, II and III. The fracture mechanics tests in modes I and III were carried out using the splitting test method by Tschegg. The fracture behaviour in mode II was analysed by the punch through test. The results confirm that the predominant concrete failure behaviour is by mode I within the interface. Experimental investigations in mode II and III have shown that cementitious materials have a tendency in their failure mode to switch to mode I because the specific fracture energy G_f of shear strain is one order of magnitude higher than for the pure tensile regime.

1 INTRODUCTION

Knowledge of the physical processes and concepts to characterize the fracture processes of cementitious composites, such as concrete, are important for civil engineers. Such knowledge facilitates decisions on constructive and material-technological steps to prevent the formation of cracks in concrete structures. It is also of interest for failure analysis purposes.

For cementitious composites the predominant failure type is mode I. There are a multitude of published papers about suitable testing procedures to obtain stable tensile failure in concrete. Most commonly used is the three-point bending test (RILEM 1983, 1985), but also often the centric or compact tension test as well as the wedge splitting test are applied. The idea of the latter test was proposed by Linsbauer & Tschegg (1986) and adopted by other research groups to characterize concrete (Rokugo 1989, Brühwiler & Wittmann 1990, Guogan et al. 1991), polymers (Tschegg et al. 1995a), wood (Stanzl-Tschegg et al. 1995) and other composite materials (Tschegg et al. 1993).

For describing the mode II fracture process in cementitious composites several models, test methods and specific geometries have been proposed, and considerable progress has been made by applying various fracture mechanical concepts in the past . A brief summary is given as follows.

Advantages and disadvantages of various shear specimen geometries and test procedures are discussed in detail by Bažant & Pfeiffer (1986), Davies et al. (1986), Ingraffea et al. (1986), Barr et al. (1987), Swartz & Taha (1990) and van Mier (1992, 1997). First approaches to determine the shear failure of concrete were generated by Bažant & Pfeiffer using a four-point shear beam test. Ingraffea et al. and Swartz & Taha obtained curved crack patterns from their four-point shear beam test. They concluded that the results of the early investigations by Bažant & Pfeiffer could not describe the simple mode II failure of concrete. Based on numerical simulations Ingraffea et al. showed that crack initiation starts from the notch in mode I and propagates with an inclined splitting tensile crack, which will lead to the complete failure of the sample. This situation is comparable to the Brazilian Test method and therefore far away from a simple mode II failure.

Davies et al. (1986) investigated the shear behaviour of concrete with the punch-through-cube specimen. An FEM analysis pertaining to this sample geometry can be found elsewhere (Davies 1988).

A comprehensive discussion of the shear failure of concrete is given by van Mier (1997). He concluded that cementitious composites possibly frac-

ture in pure mode II when the mode I failure is restricted either experimentally by multiaxial testing or by the material structure, i.e. steel fibres. Without these restrictions mixed-mode failure will occur.

Investigations focused on the mixed mode failure were carried out by Carpinteri et al. (1990), Nooru (1992) and Ohtsu et al. (1999). The RILEM Technical Comitee 89-FMT (Carpinteri & Swartz 1991) recommend a single edge notched beam using the four-point bending test method. A comprehensive summary of the state of the art on mixed-mode failure in concrete is given by Schlangen (1993).

In contrast to modes I, II and mixed-mode failure only a few experimetal results can be found about the mode III failure in cementitious composites. Comparable dispute existists on this failure mode (Bažant & Pratt 1988a,b, Yacoub-Tokatly & Barr 1989, Xu & Reinhardt 1989) as referred about the shear failure previously. Torsional tests on un-notched and notched concrete beams were applied by Bažant & Pratt, whereas Xu & Reinhardt and Ya-coub-Tokatly & Barr used cylindrical concrete specimens. The results obtained show that crack formation occurs perpendicular to the principal stresses when using unnotched samples while crack inititation as well as crack propagation of notched samples take place in the notched surface. Bažant & Pratt obtained conical failure for notched samples, which emphasises the impression that the fracture process in mode III is controlled by a tensile process mechanism on lower level.

Against this backdrop, it is obvious that in plain concrete beside the predominant tensile failure usually a mixed-mode stress distribution will be obtained if no further experimental measure is adopted. In the present study, the fracture mechanical properties of cementitious interfaces are determined in the failure modes I, II and mixed mode on the basis of the fracture energy concept (Hillerborg 1983). A new testing technique, in combination with a simple and small specimen geometry, has been developed. The test procedure permits an experimentally simple measurement of the fracture behaviour of cementitious composites in mode I, II and mixed mode with crack inititation in mode III. The main results of the tests are load versus displacement curves, which contain all the information needed to characterize the fracture behaviour of the materials for numerical calculations.

It is the aim of this paper to present a new, simple and useful method to characterize the fracture properties of cementitious composites in different failure modes which are of interest for the engineer, and to discuss first results, which were obtained with the help of the fracture energy concept.

2 EXPERIMENTAL

2.1 General

The tests in the different failure modes were performed with a mechanical spindle-driven tension-compression maschine. The load capacity of this maschine is 200 kN and the capacity of the used load cell is 2 kN. The crosshead speed was kept constant at 0.5 mm min^{-1} throughout the experiments. In respect to the splitting tests (modes I and III), the wedge angle was choosen to be 10°.

2.2 Materials

Dense, smooth limestone and porous, rough sandstone were choosen to represent the diversity of aggregates used in civil engineering structures. The rock layers or cylinders were cut or drilled out, respectively, of a block. Rock pieces were washed and sand-blasted ($R_z \approx 3 \mu m$) before casting. The matrix part was cast after the moist rock pieces had been placed into molds. Two days later, the specimens were demolded and stored in tap water for 28 days. The mechanical parameters of the rocks and the mortar is summarized in Table 1, where σ_{nbt} is the notched bending tensile strength, f_c is the uniaxial compression strength, E is the Young modulus and G_f the specific fracture energy in failure mode I.

Table 1. Mechanical Parameters of sandstone, limestone and mortar.

Sample	σ_{nbt}	f_c	E	G_f
	MPa	MPa	GPa	N/m
Sandstone	3.0	-150	11.16	162
Limestone	5.4	- 57	77.81	40
Mortar	3.5	- 35	17.00	74

The mortar mix was made of 452 kg/m^3 of PZ 375 cement, 1476 kg/m^3 of quartz sand with maximum aggregate size of 2 mm and 246 kg/m^3 of water.

The composition of the matrix materials allows one to simulate the cement mortar matrix in the vicinity of larger grains in concrete. This matrix is a complex composite material, which strength has a controlled by very small sand-cement paste interfaces. Because the length scale of the investigated macroscopic cracks is much larger, the cement mortar matrix could be treated as a uniform solid.

2.3 Mode I

The uniaxial specific fracture energy, G_f, as well as the uniaxial nominal notch tensile strength σ_{nt}, were determined from the uniaxial load-displacement curve that is created by means of the wedge splitting test (Tschegg 1986, 1991): the principle is schematically shown in Figure 1. The special merits of this

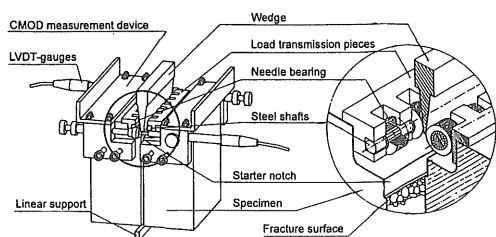simple method are the easy handling of the equipment and its reliable results.

Figure 1. Load-transmission devices for uniaxial wedge splitting test method (Tschegg 1991).

Two load-transmission pieces placed on the edges of the groove and transmit the load applied by a spindle driven testing machine to the sample. The horizontal force components cause crack propagation in the central plane of the specimen, which is additionally favoured by a narrow notch. Two inductive length measurement gauges along the lines of the horizontal force application record the crack mouth opening displacement, CMOD, depending on the wedge load. A resulting load-displacement diagram can be used to determine the specific fracture energy and the nominal notch tensile strength σ_{nt}. F_M, the force from the testing machine is split by the wedge into two forces perpendicular to the wedge flanks. Only the horizontal components (splitting forces), F_H, of these flank forces contribute to crack initiation and propagation, whereas the vertical components, F_V, cause a stabilization of the crack propagation direction (Tschegg 1986) and does not impair the results as long as the wedge angle is small enough (Tschegg 1990). The use of very small wedge angles allows for the development of horizontal forces is great enough to split the concrete cube. The relationship of the machine force, F_M, and the horizontal force, F_H, that can be deduced from the force diagram reads

$$F_H = F_M / (2 \tan (\alpha / 2)),\qquad (1)$$

providing that friction can be neglected. The multiplicative factor $1/(2 \tan(\alpha/2))$ will be denoted as wedge angle factor with $\alpha = 10°$.
The most important objective of load-transmission system is to ensure stable crack propagation conditions and to avoid energy losses due to friction processes. An increased stiffness of the testing machine and the load-transmission systems help to keep crack propagation experiments in the stable regime. A quantitative description of the stability criterion is given in Zikmunda (1992). To avoid considerable energy losses due to friction, several load-system have already been developed and published (Tschegg 1990, 1991). using a wedge with rolls or a wedge with needle bearings. Possible measurement

errors due to rolling friction are less than one percent (Tschegg 1991).
Different stone-mortar-specimen shapes may be used with the above described method, as shown schematically in Figure 2. All specimens have a rectangular groove with a starter notch. Usually cubic or rectangular shaped specimens are used as produced in the laboratory. For the determination of the size effect different ligament areas from 1830 mm^2 up to 16200 mm^2 were produced. The rectangular groove and the starter notch may be produced by inserting an appropriate mold into the cubic form during casting or by cutting with a stone saw.
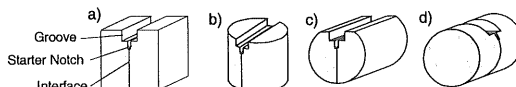

Figure 2: Specimen shapes (Tschegg 1986).

For the experimental realization the inductive length measurement gauges (LVDT) are mounted on an aluminium frame which is attached to the specimen by four screws. This frame can easily be modified for different specimen geometries. A cubic sample with attached LVDT- frame is presented in Figure 1. The analog signals registered by the testing machine are converted by means of an A/D-converter to digital information (time, machine force (F_M), cross head displacement (s), LVDT1 and LVDT2). A program has been developed to calculate all necessary parameters from load-displacement curve. The two load-displacement curves CMOD1-F_H and CMOD2-F_H (one for each inductive length gauge) are used to calculate a mean curve CMOD-F_H. Then, an integration of the mean curve can be performed.

$$G = \int_0^{\delta_{max}} F_H (\delta) \, d\,\delta,\qquad (2)$$

where G is the energy consumed for total stable separation of the specimen. The crack mouth opening displacement, CMOD, is equivalent to the δ. The specific fracture energy, G_f, is obtained by:

$$G_F = \frac{G}{A}\qquad (3)$$

where A stands for the planar projection of the fracture surface area. Using the maximum horizontal force, F_{Hmax}, a nominal notch tensile strength, σ_{nt}, can be calculated:

$$\sigma_{nt} = \frac{F_{H\,max}}{A} \cdot \frac{M}{W}\qquad (4)$$

where M describes the moment and W is the moment of resistance. Further details of the calculation of σ_{nt} can be found in Tschegg 1991 and Tschegg & Stanzl 1991.

The obtained load-displacement curve provides additional information for FEM simulation. It can also be used for a calculation for the strain softening behavior of concrete (Roelfstra 1985).

2.4 Mode II

A loading arrangement to determine shear failure in conrete was published by Watkins (1983) and Davies (1986). The presented "punch-through-cube" test was modified into an improved loading device, the "punch-through-cylinder" test, for this study. Special cementitious interface specimens containing cylindrical inserts made of sandstone and limestone in a rectangular were used for the fracture mechanical characterization of the behaviour of cementitious interfaces in the shear mode. The geometry of the shear test device with the rectangular interface shear specimen, which is double-notched on both the top and the bottom side of the specimen, are shown in Figure 3a,b.
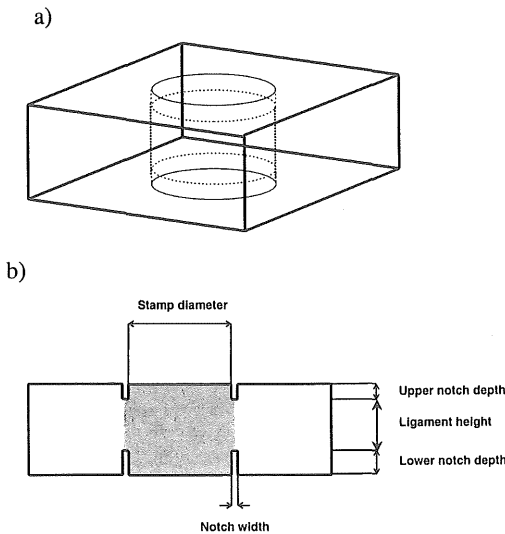
a)

b)

Figure 3: a) Mode II specimen , consisting of rock specimen insert which is embedded in mortar. b) specimen dimensions.

The starter notch was produced by a thin metal cylinder around the rock specimens. The groove was generated by a rubber covering both the rock and the metal cylinders. It should be noted that the rubber did not cover the metal cylinder completely. The rock specimens were inserted into the rectangular form during casting of the mortar. The structure and geometry of the rock inserts are shown in Figure 4.

The ligament height was choosen between 10 and 40 mm. After hardening of the mortar the rubber covering and the metal cylinders are removed from the notches. The notches have a sharp shape which is suitable for mode II size effect testing.

Figure 4. Structure and geometry of rock inserts.

The specimen is placed on to a U-form (Fig. 5) support provided with a simply designed rig in order to ensure that a punch-through shear mechanism is maintained during testing. The load, F, is applied vertically over a stamp using a stiff tensile testing machine in combination with a force-reversal arrangement, in which the punch-through device is placed on the U-form support. On the specimen surface a flat parallel metal laminar with approx. 5mm thickness and a spherical calotte were applied as load transmission equipment to ensure a homogeneous load distribution (Fig. 5).
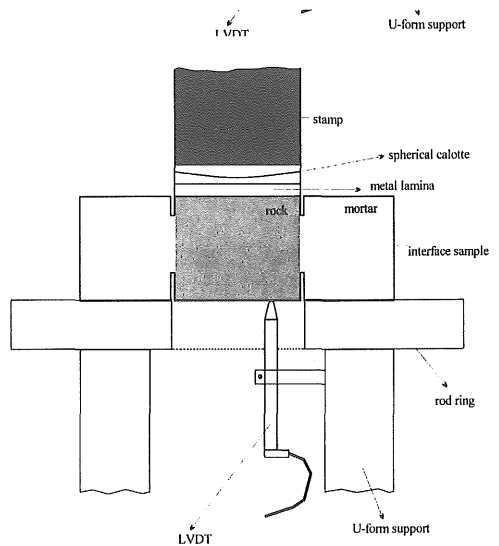

Figure 5. Shear test device "punch-through-cylinder" with interface specimen in the test position.

For the experimental realization of the "punch-through-cylinder" test an inductive length measurement gauge (LVDT) is mounted on the U-form support with its measuring tip arranged acentric to the cylindrical insert of the specimen. During the measurements, both the vertical displacement, δ, of the compressive plate and applied load, F, were registered by the testing machine as analog signals and

456

afterwards converted by means of an internal 16 bit A/D-converter to digital information, which is stored in ASCII-format on a hard disk. During testing, the crack propagates under a stable crack growth mechanism, providing that the testing machine including the load transmission equipment are stiff and strong enough.

The non-linear material behaviour of cementitious composites is based on the fracture process zone which contains microcracks and mechanical interlock phenomena. If a certain deformation level is reached, friction actions predominate in failure mode II. To describe this nonlinearity, the load-displacement curve is divided in three different areas: crack initiation energy G_i is characterized by the area A-B-C, crack propagation ends by point E and friction between the fractured surfaces is described by the cross-hatched area below the curve. Plastic deformations are observable before maximum load (point B) is obtained, which is defined as crack initiation energy. Crack propagation and friction forces between the mode II interfaces consume energy, which is represented by the post-peak behaviour of the load-deformation diagram. For the calculation of the softening behaviour of the interface and the friction during crack propagation numerous fracture models were applied by Tschegg et al. (1998). The transition point of the decreasing branch to the constant friction part of the load-displacement curve is critical to evaluate. In this paper, the following model was chosen, which is shown in Figure 6.
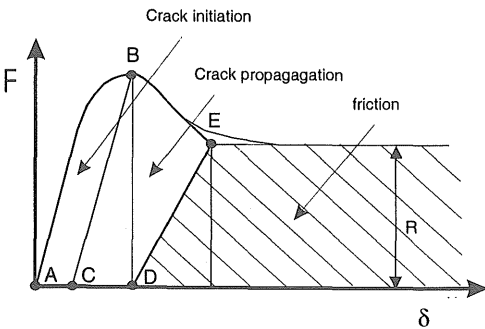

Figure 6. load-displacement diagram for mode II

The softening of the interface (line B-E) increased proportionaly with the friction action (D-E) after the introduction of the crack propagation at F_{max} (point B). The asymptotic behaviour of the softening branch (B-E) is replaced by a tangent. The cross point E represents the end of the crack propagation. In case of a sample release at point E the softening branch would cross point D. The area under the experimentally measured load-displacement curve (F/δ curve) is considered to be equal to the total work of fracture needed to carry out the punch-through test

completely, and is denoted by the term "fracture energy, G" (see relation (2)). The specific fracture energy, G_f, can be calculated in according to relation (3) where A is the complete fracture surface or the shear area and G_1 is the elastic fracture work. Further models were developed by Tschegg et al. (1998), where: (i) the transition point E is moved further down on the curve which leads to a higher fracture energy; (ii) point D is moved to the right to obtain a segment D-E parallel to the elastic pre-peak behaviour, which results in a higher fracture energy as well.

2.5 Mode III

The loading arrangement to determine the fracture behaviour of cementitious interfaces in antiplane shear failure (mode III) is shown in Figure 7.
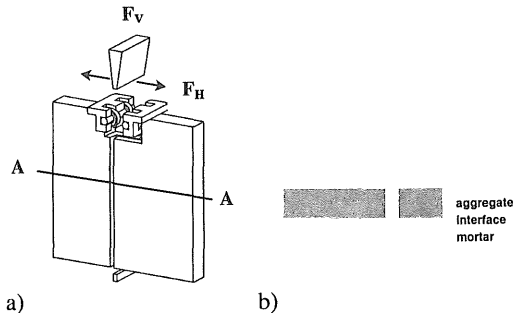

a)   b)

Figure 7. a) Antiplane shear test device with specimen in the test position, b) specimen on plan view

The loading device is comparable to the loading equipment of the mode I test. All samples have a groove with a starter notch similar to that of the mode I specimens, but pependicularly oriented to the wedge and in longitudinal axis respectively. This starter notch is limited by marginal arranged side notches, (Fig. 7) which can be produced as "Chevron-notches" to obtain a better crack inititation.

A compression force on the wedge generates the horizontal load, which shears off the specimen in mode III, starting from the starter notch. During the crack propagation in mode III, some mode I failure is assumed. Only a small part of elastic energy is stored in the loading device and the specimen. Thus, stable crack propagation is expected. In contrast to the mode I experiments, length measurements were realized by the video extensometer technique. Testing procedure, data collection and evaluation were carried out in the same way as described for mode I failure tests. The specimen geometry is comparable to that of the mode I tests; the ligament area varies between 90 and 1400 mm.

3 RESULTS

A summary of the experimental results obtained from interface samples in different failure types are listed in Table 2.

Table 2. Results from the fracture mechanical testing in mode I, II and III of cementitious interfaces with sandstone and limestone aggregates.

Sample	failure mode	no. of tests	σ_{nbt}, τ_{max}	G_f
			GPa	N/m
Sandstone	I	5	1.2 ± 0.2	9.5 ± 2.4
	II	3	2.9 ± 0.7	467.0 ± 115.0
	III	5	2.2 ± 0.0	29.4 ± 0.0
Limestone	I	8	1.3 ± 0.4	6.6 ± 3.4
	II	7	3.1 ± 0.4	151.0 ± 35.0
	III	2	4.0 ± 0.1	21.1 ± 2.2

Mean values with standard derivation σ_s of the notched bending tensile strength σ_{nbt} obtained from the mode I and II tests, of the shear strength τ_{max} determined by mode II experiments and of the specific fracture energy G_f in the three different failure modes are given in this table. It should be noted that in most cases mixed mode failure took place at the mode III experiments with the sandstone aggregate due to the anisotropic material structure developed during sedimentary petrogenesis of the rock in the past. Examples of sandstone and aggregate samples following fracture in the antiplane shear mode (mode III) are shown in Figure 8. Mixed mode failure in the case of the sandstone interface specimen is obvious.
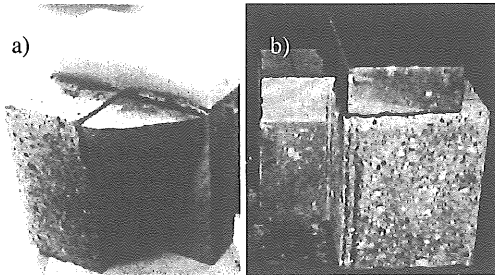

Figure8. Fractography of cementitious interfaces specimens of a) sandstone and b) limestone aggregates after antiplane shear test.

Whenever heterogeneous materials are tested, "size effects" are well known to occur, and hence, must be investigated in detail. Significant size effects could only be found within the shear experiments. Experimental data of sandstone and limestone shear tests are listed in Table 3 where A_{lig} is the fractured area. Typical load-displacement curves (F/δ) of limestone aggregate interface specimens for mode I and III are shown in Figure 9. While for mode I and III fracture the F/δ curves of limestone interface specimens are

comparable to that of sandstone, the material response in shear mode failure is quite different (Fig.10).

Table 3. Size effect data in cementitious interface specimens of sandstone and limestone aggregates in failure mode II.

Sample	test no.	A_{lig}	τ_{max}	G_f
		mm^2	GPa	N/m
Sandstone	1	1744	2.9	457.0
	2	2592	3.7	588.0
	3	2639	2.2	358.0
Limestone	1	1696	2.8	177.0
	2	2827	2.7	115.0
	3	1790	3.9	177.0
	4	3675	3.0	148.0
	5	3679	2.9	181.0
	6	1037	3.3	130.0
	7	1030	3.4	132.0

4 DISCUSSION

As pointed out in Section 1, the main problem of fracture mechanical testing on cementitious interfaces is the determination of the crack tip and the crack length with sufficient accuracy. Several fracture mechanical concepts, which have been used so far for the fracture mechanical characterization of cementitious composites (e.g., the K-, G-, J- or R-concept), require explicitly the exact crack length for fracture mechanical calculations. In comparison to these concepts, no accurate determination of the exact crack length and of the crack elongation is needed for fracture mechanical calculations using the fracture energy concept. A further advantage lies in the fact that the recorded (F/δ) curve contains all the information which is needed for an application of the fracture energy concept. Starting from these curves, finite element calculations allow one to determine complete stress-strain curves, which are needed for a full material characterization and for design purposes. On the other hand, one of the main disadvantages of the fracture energy concept lies in the fact that the experimentally measured load-displacement curves (and consequently the specific fracture energy, G_f) could depend on the sample geometry, especially if the sample size is too small in comparison to the damage zone, which is being formed during the fracture process. Under these circumstances, the fracture energy - and consequently the calculated material parameters for failure mode II given in Table 2 can not be called "characteristic material parameters," which must, of course, be independent of sample geometry and size. Therefore, extensive scaling experiments have been made and only the punch-through shear specimen have showed a significant size dependency. The load-displacement curves (F/δ) of sandstone and limestone aggregate interface specimens, measured in three different

failure modes should be discussed in detail. Because of the lower specific energy, G_f, in mode I compared to mode II and mode III respectively, resulting from Figures 9, 10, tensile failure will be the predominant failure type in cementitious interfaces.
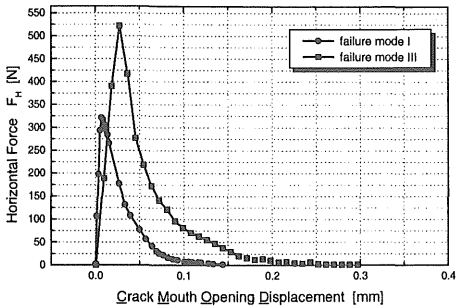

Figure 9. Load-displacement curves (F/δ) of limestone-mortar interface specimens for failure mode I and III (A_{lig} I ≈ A_{lig} III).

This is obvious comparing results of G_f in tensile and shear mode, whereas only small but statistically significant differences in G_f values exist between mode I and III. This is due to the experimental setup of the antiplane shear test. Hence, after crack initiation in mode III, crack opening in mode I is possible resulting in mixed-mode failure of the interface specimen.
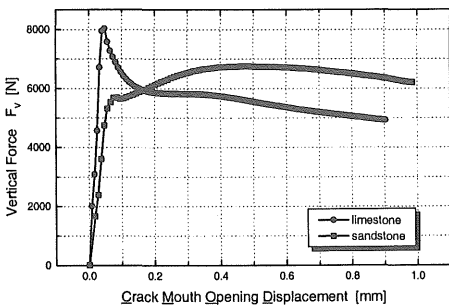

Figure 10. Load-displacement curves (F/δ) of limestone and sandstone-mortar interface specimens for failure mode II (sandstone-ligamant area ≈ limestone-ligament area).

As mentioned by Bažant & Pratt (1988), conical failure for notched samples emphasise the impression that the fracture process in mode III is controlled by a tensile process mechanism on a lower. In our experiments no clear conclusion about tensile process mechanisms can be made because mixed-mode failure took place in the sedimentary rock structure which acts as a prime crack path.

As pointed out in Section 2, the determination of the specific fracture energy, G_f, in failure mode II was done by using a specific fracture model. As can

be seen from Figure 10, different material responses could be obtained from shear test of limestone and sandstone aggregate interface specimens. Before reaching the maximum load, linear elastic material behaviour prevails at both material interfaces. Afterwords, the softening behaviour of these curves can be distinguished. Both aggregate interface specimens show friction action, which increases linear with progressive crack propagation, but while the post-peak behaviour of limestone decreases during this process that of sandstone increases. The origin of this opposite fracture behaviour could be found in the microfabric of the rock materials. Limestone is a fine granular material of calcite crystals within a lime matrix whereas sandstone consists of coarse quartz crystals surounded by lime. The rigidity of the quartz in comparison to the limestone effects the increasing post-peak behaviour due to more emphasized micro-keying and bridging phenomena. Therefore, the specific fracture energy of sandstone is significantly higher than the G_f value of limestone in failure mode II.

5 CONCLUSION

The fracture mechanical characterization of interfaces in cementitious composites in shear mode (mode II) is of considerable interest for various applications. In the past, several different sample geometries have been proposed for mode II tests on concrete, but no test method has received general acceptance. In this paper, a shear test technique has been proposed for the characterization of fracture properties in shear mode (mode II), which is based on the fracture energy concept. With finite element calculations, complete stress strain curves can be determined from the load-displacement curves. The main aspects of the test method as well as the results of tests obtained on limestone and sandstone aggregate interface specimens, may be summarized as follows:

1. The test methods are experimentally simple. The loading device and the sample geometry are small and well suited for tension-compression test machines.
2. The fracture energy concept does not require a knowledge of the exact crack length. The recorded load-displacement curves contain all the information needed for a full material characterization.
3. Two different fracture models were proposed for determination of fracture mechanical parameters of cementitious composites in shear mode.
4. The measured load-displacement curves show linear-elastic material behaviour at the beginning. The post-peak behaviour (strain-softening area) varies depending on the failure mode and the used rock material.

5. Scaling experiments have shown a dependence of the specific fracture energy, G_f, on the specimen dimensions in case of the shear mode tests. Fractographic investigations have shown a mixed-mode failure within the sandstone when antiplane shear load is applied due to the sedimentary petrofabric of the aggregate material.
6. The aggregate–cement matrix interface acts like a weak link in concrete. The predominant failure type of interfaces in cementitious composites is mode I. Significant higher G_f values were obtained for shear failure.
7. It is remarkable that the relations of the fracture energies G_f of mode I/II/III are as follows:
sandstone: $(G_f)_I : (G_f)_{II} : (G_f)_{III} = 9,5 : 467 : 29,4$
limestone: $(G_f)_I : (G_f)_{II} : (G_f)_{III} = 6,6 : 151 : 21,1$

ACKNOWLEDGEMENTS

REFERENCES

Barr, B. & Hasso, A.B.D. & Khalifa, S.M.A. 1987. A study of mode II shear fracture of notched beams, cylinders and conces. In S.E. Swartz & S.P. Shah (eds), *Fracture Mechanics of Concrete and Rock*: 370. London: Elsevier.

Bažant & Pfeiffer 1986. Shear fracture tests of concrete. *Materials and Structures* 19: 111.

Bažant & Pratt, P.C. 1988. Measurements of mode III fracture energy of concrete. *Nuclear Engineering Design* 106: 1.

Carpinteri, A. & Ferrara, G. & Melchiorri, G. & Valente, S. 1990. The four point shear test on single edge notched specimen : an experimental and numerical analysis. In D. Firrao (ed), *Fracture Behaviour and Design of Concrete Structures*: 667. Warley UK: EMAS.

Carpinteri, A. & Swartz, S.E. 1991. Mixed-mode crack propagation in concrete. *Chapter 3*. London: Chapman & Hall.

Davies, J. & Morgan, T.C. & Yim, A.W. 1986. The finite element analysis of specimens giving a mode II type of failure. In F.H. Wittmann (ed) & H. Mihashi & Takahshi, H. (eds), *Fracture Toughness and Fracture Energy of Concrete*: 209-212. Rotterdam: Balkema.

Davies, J 1988. *International Journal of Cementitious Composites & Lightweight Concrete* 10:3.

Guogan, Z. & Hui, J. & Shilang, X. 1991. Study of fracture behaviour with wedge splitting test method. In J.G.M. van Mier & J.G. Rots & A. Bakker (eds), *Fracture Process in Concrete, Rock and Ceramics*: 789-798. London: E&FN Spon.

Hillerborg, A. 1983. Analysis of a single crack. In F.H. Wittmann (ed), *Fracture Mechanics of Concrete*: 223-249. Amsterdam: Elsevier.

Ingraffea, A.R. & Panthaki, M.J. 1986. Analysiws of shear fracture tests of concrete beams. In C. Meyer & H. Okamura (eds), *Finite Element Analysis of Reinforced Concrete Structures*: 151. New York: ASCE.

Linsbauer, H. & Tschegg, E.K. 1986. Die Bestimmung der Bruchenergie von zementgebundenen Werkstoffen an Würfelproben. *Zement und Beton* 31(1): 38-40.

Nooru, M 1992. *Mixed-mode fracture of concrete: an experimental approach*. PhD thesis, Delft University of Technology, NL.

Ohtsu, M & Kaminaga, Y. & Munwam, M. 1999. Experimental and numerical crack analysis of mixed-mode failure in concrete by acoustic emission and boundary element method. *Construction and Building Materials* 19: 57-64.

RILEM 1985. Determination of the fracture energy of mortar and concrete by means of three-point bending tests on notched beams. *Materials and Structures* 18:287-290.

Roelfstra, P. E. 1985. *Numerical concrete*. PhD thesis, Swiss Federal Institute of Technology,Lausanne.

Rokugo, K. & Iwasa, M. & Suzizki, T. & Koyanagi, W. 1989. Testing method to determine tensile strain softening curve and fracture energy of concrete. In F.H. Wittmann & H. Mihashi & Takahshi, H. (eds), *Fracture Toughness and Fracture Energy of Concrete*: 153-163. Rotterdam: Balkema.

Schlangen , E. 1993. *Experimental and numerical analysis of fracture process in concrete*. PhD thesis, Delft University of Technology, NL.

Stanzl-Tschegg, S.E. & Tan, D.M. & Tschegg, E.K. 1995. New splitting method for wood fracture characterization. *Wood Science and Technology* 29: 31-50.

Swartz, S.E. & Taha, N.M. 1990. Mixed mode crack propagation and fracture in concrete. *Journal of Fracture Engineering Mechanics* 35:137.

Tschegg, E.K. 1986. *Equipment and appropriate specimen shapes for tests to measure fracture values*. Austrian patent No. A-233/86, 390 328. Patent application 31.01.1986.

Tschegg, E.K. 1990. *Load transmission equipment for fracture tests in brittle and ductile materials*. Austrian patent No. A-48/1990, 396 997. Patent application 11.01.1990.

Tschegg, E.K. 1991. New equipment for fracture tests on concrete. *Materialprüfung* 33(11-12): 338-342.

Tschegg, E.K. 1993. New testing method to characterize mode I fracturing of asphalt aggregate mixtures. In J.M. Rigo, R. Degeimbre & L. Franken (eds), *Reflective Cracking in Pavements*: 236-270. London: E&FN Spon.

Tschegg, E.K. & Humer, K. & Weber, H.W. 1995a. Mode II fracture tests on fibre-reinforced plastics. *Journal of Material Science* 30: 1251-1258

Tschegg, E.K. & Jamek, M. & Surberg, C.H. 1998. Stein-Mörtel Verbunde in Mode I/II/III. Prüfbericht, Hilti AG.

Tschegg, E.K. & Stanzl, S.E. 1991. Adhesive power measurements of bonds between old and new concrete. *Journal of Materials Science* 26: 5189-5194.

Van Mier, J.G.M. 1992. Shear fracture in slurry infiltrated fibre concrete (sifcon). In H.W. Reinhardt & A.E. Naaman (eds), *High Performance Fibre Reinforced Cement Composites*: 348. New York: Chapman & Hall.

Van Mier, J.G.M. 1997. *Fracture Process of Concrete*. New York: CRC Press.

Watkins, J. 1983. *International Journal of Fracture* 23: 135.

Xu, D. & Reinhardt, H.W. 1989. Softening of concrete under torsional loading. In S.E. Swartz & S.P. Shah (eds), *Fracture Mechanics of Concrete and Rock*: 39. London: Elsevier.

Yacoub-Tokatly, Z. & Barr, B. 1989. Mode III fracture – a tentative test geometry. In S.E. Swartz & S.P. Shah (eds), *Fracture Mechanics of Concrete and Rock*: 596. London: Elsevier.

Zikmunda, W. 1992. *Bruchmechanische Charakterisierung des Haftvermögens zementgebundener Werkstoffe*. PhD thesis, Vienna University of Technology, Austria.